Autoimmunity, hypogammaglobulinemia, lymphoproliferation and mycobacterial disease in patients with dominant activating mutations in *STAT3*

Emma M. Haapaniemi,[1] Meri Kaustio,[2] Hanna L.M. Rajala,[3] Arjan J. van Adrichem,[2] Leena Kainulainen,[4] Virpi Glumoff,[5] Rainer Doffinger,[6] Heikki Kuusanmäki,[2] Tarja Heiskanen-Kosma,[7] Luca Trotta,[2] Samuel Chiang,[8] Petri Kulmala,[5,9] Samuli Eldfors,[2] Riku Katainen,[10] Sanna Siitonen,[11] Marja-Liisa Karjalainen-Lindsberg,[11] Panu E. Kovanen,[12] Timo Otonkoski,[13] Kimmo Porkka,[3] Kaarina Heiskanen,[14] Arno Hänninen,[15] Yenan T. Bryceson,[8] Raija Uusitalo-Seppälä,[16] Janna Saarela,[2] Mikko Seppänen,[17] Satu Mustjoki,[3] and Juha Kere[1,18]

[1]Folkhälsan Institute of Genetics and Research Programs Unit, Molecular Neurology, University of Helsinki, Helsinki, Finland;
[2]Institute for Molecular Medicine Finland, University of Helsinki, Helsinki, Finland;
[3]Hematology Research Unit Helsinki, Department of Hematology, University of Helsinki and Helsinki University Central Hospital Cancer Center, Helsinki, Finland;
[4]Department of Pediatrics and Department of Medicine, Turku University Hospital, Turku, Finland
[5]Department of Medical Microbiology and Immunology, Medical Research Center Oulu, Oulu University Hospital and University of Oulu, Oulu, Finland;
[6]Department of Clinical Biochemistry and Immunology, Addenbrooke's Hospital and National Institute for Health Research (NIHR), Cambridge Biomedical Research Center, Cambridge, United Kingdom
[7]Department of Pediatrics, Kuopio University Hospital, Kuopio, Finland;
[8]Center for Infectious Medicine, Department of Medicine, Karolinska Institutet, Stockholm, Sweden;
[9]Department of Pediatrics, Medical Research Center Oulu, Oulu University Hospital and University of Oulu, Oulu, Finland
[10]Department of Medical Genetics, Genome-Scale Biology Research Program, Institute of Biomedicine, University of Helsinki, Helsinki, Finland;
[11]Laboratory Services (HUSLAB), Helsinki University Central Hospital, Helsinki, Finland;
[12]Department of Pathology, Helsinki University Central Hospital, Helsinki, Finland;
[13] Children's Hospital, Helsinki University Central Hospital, Helsinki, Finland, and Research Programs Unit, Molecular Neurology, University of Helsinki, Helsinki, Finland;
[14] Children's Hospital, Helsinki University Central Hospital, Helsinki, Finland,
[15]Department of Medical Microbiology and Immunology, University of Turku, Turku, Finland
[16]Department of Infectious Diseases, Satakunta Central Hospital, Pori, Finland
[17]Immunodeficiency Unit, Department of Medicine, Helsinki University Central Hospital, Helsinki, Finland;
[18]Department of Biosciences and Nutrition, and Center for Innovative Medicine, Karolinska Institutet, Stockholm, Sweden

Running title: Germline *STAT3* mutations in IPEX-like syndrome

Corresponding authors

Satu Mustjoki, M.D.   Mikko Seppänen, M.D.
Hematology Research Unit Helsinki   Immunodeficiency Unit
Helsinki University Central Hospital   Division of Infectious Diseases
Haartmaninkatu 8   Helsinki University Central Hospital
P.O. Box 700   P.O.Box 348
FIN-00290 Helsinki, Finland   FI-00290 Helsinki, Finland
e-mail: satu.mustjoki@helsinki.fi   e-mail: mikko.seppanen@hus.fi
Tel +358 9 471 71898   Tel +358 9 471 75923
Fax +358 9 471 71897   Fax +358 9 471 5945

Janna Saarela, M.D.
Institute for Molecular Medicine Finland
University of Helsinki
Tukholmankatu 8
P.O. Box 20
FIN-00290 Helsinki, Finland
e-mail: janna.saarela@helsinki.fi
Tel +358 9 191 25755

Word count (text): 3954
Word count (abstract): 148
Figure count: 3
Table count: 3
Reference count: 29

IMMUNOBIOLOGY   Submitted: 4/15/2014
                                2nd revised version submitted: 3/10/2014

Key points

- Germline activating STAT3 mutations were detected in three patients with autoimmunity, hypogammaglobulinemia and mycobacterial disease.
- T cell lymphoproliferation, deficiency of regulatory and Th17 T cells, NK cells, dendritic cells and eosinophils were common.

Abstract

The signal transducer and activator of transcription (STAT) family of transcription factors orchestrate hematopoietic cell differentiation. Recently, mutations in *STAT1*, *STAT5B*, and *STAT3* have been linked to development of IPEX-like syndrome. Here, we immunologically characterized three patients with *de novo* activating mutations in the DNA binding or dimerization domains of *STAT3* (p.K392R, p.M394T and p.K658N, respectively). The patients displayed multi-organ autoimmunity, lymphoproliferation, and delayed-onset mycobacterial disease. Immunologically, we noted hypogammaglobulinemia with terminal B cell maturation arrest, dendritic cell deficiency, peripheral eosinopenia, increased double-negative (CD4$^-$CD8$^-$) T cells, and decreased NK, Th17, and regulatory T cell numbers. Notably, the patient harboring the K392R mutation developed T cell LGL leukemia at age 14. Our results broaden the spectrum of phenotypes caused by activating *STAT3* mutations, highlight the role of STAT3 in the development and differentiation of multiple immune cell lineages, and strengthen the link between the STAT family of transcription factors and autoimmunity.

Keywords

Introduction

Primary immunodeficiency (PID) syndromes are a heterogeneous group of diseases with variable manifestations, including autoimmunity. The most characteristic early-onset autoimmunity syndrome is Immunodysregulation–Polyendocrinopathy–Enteropathy–X-linked (IPEX) syndrome, which leads to fatal autoimmunity unless treated with stem cell transplantation. IPEX is associated with recessive mutations in *FOXP3,* encoding a transcription factor essential for regulatory T cell (T_{reg}) development.[1] Other genetic causes include mutations in *CD25*, *STAT1*, *STAT5B*, and *ITCH.*[2-4]

The signal transducer and activator of transcription (STAT) transcription factors are widely expressed in hematological and other cell types, and mutations causing either gain or loss of STAT activity have been associated with PID syndromes.[2,5-8] The cytokine-receptor–Janus kinase (JAK)–STAT pathway has an important role in the regulation of the immune system, and different STAT family members have been ascribed specific roles in determining T cell differentiation in response to certain cytokines. Generally, Th1 cell differentiation is mediated by the IFN-γ–STAT1 and IL-12–STAT4 axis, Th2 differentiation by the IL-4–STAT6 axis, Th17 by the IL-6–STAT3 axis, and commitment to T_{reg} pathway by the IL-2–STAT5 axis.[9,10] Consequently, mutations in *STAT* genes lead to variable clinical presentations, ranging from susceptibility to viral infections and mycobacterial disease to multi-organ autoimmunity.[2,5-8] As an example, dominant-negative germline mutations in *STAT3* cause Hyper-IgE-syndrome (HIES),[5,6] whereas recently discovered somatic activating *STAT3* mutations have been found in 40-70% cases of large granular lymphocytic (LGL) leukemia, a neoplastic disease accompanied by autoimmune manifestations such as rheumatoid arthritis and autoimmune cytopenias.[11-13]

We evaluated three patients who carried germline heterozygous activating *STAT3* mutations, two of which were recently published as part of a larger cohort featuring five STAT3-gain-of-function patients.[14] The two patients presented with aggressive multi-organ autoimmunity and lymphoproliferation, including pediatric LGL leukemia. The third patient first described here had late-onset autoimmune manifestations and developed disseminated mycobacterial disease in late adolescence. Immunologically, we noted hypogammaglobulinemia with terminal B cell maturation arrest, dendritic cell deficiency, peripheral eosinopenia, increased double-negative (CD4⁻CD8⁻) T cells, and low NK, Th17, and regulatory T cell counts.

Methods

Study patients

We evaluated two patients characterized by early-onset autoimmunity and growth failure previously published as part of a larger autoimmunity cohort[14] and one with delayed-onset disseminated non-tuberculous mycobacteriosis (Table 1 and Figure 1, detailed case descriptions are in Supplementary appendix). Patient 1 is a 17-year old female born full term without complications. She was first brought to medical attention at 12 months of age for diarrhea and abdominal pain caused by autoimmune enteropathy. At the age of two, she developed generalized, livedo-like exfoliating dermatitis (Figure 1). At age six, marked and progressive lymphadenopathy and splenomegaly were noted, with lymph node biopsy showing polyclonal CD4^{+} T cell expansion. At age 10, she suffered from sicca and was diagnosed with bilateral posterior uveitis with cystic macular edema that has since led to severe visual impairment. She also experienced recurrent autoinflammatory episodes with high fever, sterile pleuritis, and serositis with concomitant rise in inflammatory markers. Her growth was retarded and alternated between -2 SD to -4 SD. Due to recurrent upper respiratory tract infections since birth, multiple tympanostomies and functional endoscopic sinus surgery were performed at age 11. From early school age, the patient has suffered from reversible bronchoconstriction and at age 12, high-resolution computer tomography showed moderate bronchiectasis. Immunoglobulin replacement therapy was then introduced to treat mild unspecific hypogammaglobulinemia with positive response in her rate of infections. Recently, the patient developed rapidly worsening cryptogenic organizing pneumonia requiring invasive ventilation and high-dose steroids. At the time of sampling, she was using systemic tacrolimus and corticosteroid medication and was on intravenous immunoglobulin replacement therapy.

Patient 2 is a 15-year-old female who was born small for gestational age at week 34 (1380 g/40.5 cm/30.5 cm, -5 SD). At birth, she was diagnosed with neonatal diabetes mellitus with extremely high insulin (IAA), glutamate decarboxylase (GADA) and islet cell (ICA) autoantibodies.[15] The patient suffered from multiple early-onset allergies. Despite initial height catch-up, worsening idiopathic growth failure with gradual deterioration to -7 SD was noted. At 12 months, she was diagnosed with coeliac disease. The pancreas was rudimentary in the abdominal magnetic resonance imaging. She developed desquamative interstitial pneumonitis in infancy that later progressed to pulmonary fibrosis. At school age, she suffered from recurrent pneumonias. Gradually worsening and severe unspecific hypogammaglobulinemia was noted, leading to immunoglobulin replacement therapy at age 12. At age 14, the patient developed megaloblastic

5

anemia (Mean corpuscular volume 101, Hemoglobin 6.0 g/L) with clonal T cell large granular lymphocyte (LGL) proliferation and was subsequently diagnosed with T cell LGL leukemia. Recently, she developed relapsing thrombosis of right internal carotid artery and suspected vasculopathy. She is currently dependent on weekly red blood cell transfusions. At the time of sampling she was using systemic tacrolimus, high-dose steroid and mycophenolate mofetil and was on intravenous immunoglobulin replacement therapy.

Patient 3 is a 22-year-old female with normal growth and development. Reactions to vaccinations, including the BCG vaccination, were normal. In early childhood she had several ear infections leading to tympanostomy and adenotomy. At the age of 17 the patient presented with prolonged diarrhea and abdominal pain caused by lymphocytic colitis, which was successfully treated with peroral budesonide and loperamide. She also experienced episodes of marked immune thrombocytopenia and has reported swelling and stiffness in small joints. At 19, the patient developed persistent fever due to *Mycobacterium avium* pneumonia and was also diagnosed with antibody deficiency. The patient received immunoglobulin replacement therapy and standard treatment for mycobacterial infection with good response. At age 21, the patient developed fistulating cervical lymphadenitis with concomitant mediastinal and axillar lymphadenopathy. *M. avium* was found in lymph node biopsy, bone marrow and feces. The patient is currently being treated with a combination of clarithromycin, ethambutol and levofloxacin as well as intravenous immunoglobulin. At the time of sampling, no immunomodulatory drugs were used.

The study was conducted in accordance to the principles of the Helsinki Declaration and was approved by the Helsinki University Central Hospital Ethics Committee. Written informed consent was obtained from all patients and healthy controls.

DNA and RNA extraction and selection of γδ T cells

Genomic DNA was extracted from freshly sorted T cell fractions, EDTA blood samples or salivary samples using Qiagen FlexiGene DNA kit (Qiagen), Gentran puregene kit (Qiagen) or OraGene DNA Self-Collection Kit (OGR-250, DNA Genonek). RNA was extracted from heparin blood samples with the Qiagen miRNeasy kit (Qiagen). The $CD3^+\gamma\delta^+$ cell fraction (patient 2) was sorted from fresh PMNCs by flow cytometry using antibodies against CD3, CD8, CD3, TCR-αβ, and TCRB-γδ (BD Biosciences).

Exome sequencing from whole blood, saliva and γδ T cell fractions and validation of candidate mutations

Whole exome sequencing was performed in Institute for Molecular Medicine Finland (FIMM) sequencing core facility, Science for Life laboratory Stockholm, and University of Exeter according to established laboratory protocols. The read mapping, variant calling and filtering steps for somatic and germ-line variants were performed as described previously.[12,16] The candidate mutations were verified by capillary sequencing from blood and salivary DNA samples. The primers are listed in Supplementary table S1.

STAT3 luciferase reporter assay and analysis of Y705-pSTAT3 in transiently transfected cells

The K658N, K392R, and M394T mutations were introduced into wild type (WT) *STAT3* sequence in pDEST40 vector using Phusion Site Directed Mutagenesis Kit (Thermo Scientific) (primer sequences are in Supplementary table S1). The STAT3 luciferase reporter assay and pSTAT3^{Y705} western blotting were performed as previously described.[12] Briefly, HEK293 cells stably expressing a STAT3-responsive firefly luciferase reporter were plated onto 96 well plates at 15,000 cells/well and 6 h after plating, transfected with empty, WT or mutant STAT3 plasmids. The following day, the cells were starved for 3 h and subsequently mock treated or stimulated with IL-6 for 3 h. The luciferase activity was measured with One-Glo Luciferase Assay System (Promega) according to manufacturer's recommendations. Equal plasmid transfection and STAT3 phosphorylation were assessed by western blotting using parallel-derived whole cell lysates. Mouse anti-STAT3 (9139, Cell Signaling Technology 1:1000), polyclonal rabbit anti-human pSTAT3^{Y705} (9131, Cell Signaling Technology 1:1000), and mouse anti-α-tubulin (T902, Sigma-Aldrich 1:1000) were used as primary antibodies. Secondary antibodies were goat anti-rabbit IRDye 800 (Li-cor Odyssey 926-32211 - 1:1:15.000) and goat anti-mouse IRDye 680 (Li-cor Odyssey 926-32220 - 1:1:15.000). Statistical significance was calculated using 2-way ANOVA.

Immunophenotyping of T, B, and NK cell subsets and peripheral blood Y705-pSTAT3 analysis

Fresh EDTA-blood samples or PBMNCs were used for B and T lymphocyte immunophenotyping using 4- or 6-color flow cytometry panel with mAbs against the surface antigens IgM, IgD, CD3, CD4, CD8, CD16⁄56, CD19, CD21, CD27, CD33, CD34, CD38, CD45, CD56, CD57, CD133, HLA-DR, CD62L, CD45RA, CD45RO and Ki-67 (BD Biosciences).[17] The memory status of T

7

cells was studied with the antibody panel including anti-CD45 (clone 2D1), -CD3 (SK7), -CD4 (SK3), -CD45RA (GB11) and -CCR7 (150503) (R&D Systems).[17] Phosphorylated STAT3 (pSTAT3^{Y705}) expression was assessed using Y705-pSTAT3-PeCF594 (cat. 562673, BD Biosciences). For T_{reg} analysis, anti-CD4-PerCP (BD345770), -CD25-APC (BD555434) and -CD127-PE (BD557938) mAbs (BD Biosciences) were used for surface staining and FOXP3 Alexa fluor 488 mAb (320112, BioLegend) for intracellular staining (eBioscience).

For phenotyping of IL-17 positive Th17 cells, fresh PBMNCs were stimulated for 16 h with anti-CD3/anti-CD28 beads (Life Technologies) in the presence of Brefeldin A (Sigma-Aldrich). Thereafter, the cells were fixed, permeabilized and stained with anti-CD4 (Alexa Fluor 488 BD557695), CD69-APC (BD555533), and IL-17A-PE (BD560486) (BD Biosciences). Samples from patients 2 and 3 were additionally stained with CD161-APC-Cy7 (BD557756) (BD Biosciences). Samples were analyzed with FACSAria II or FACSCanto II flow cytometer and FACSDiva (BD Biosciences) or FlowJo softwares (TreeStar Inc).

Evaluation of T_{reg} suppressor capacity and NK and CD3$^+$CD8$^-$-mediated cell cytotoxicity

CD4$^+$CD25$^+$CD127$^-$ T_{reg} cells were sorted from whole blood using Human CD4+ T Cell Enrichment Cocktail (Stemcell Technologies) and fluorescence-activated cell sorting with mAbs against CD4-PerCP (BD345770), CD25-APC (BD555434) and CD127-PE (BD557938) (BD Biosciences). The cells were incubated for 6 days with CFSE-labelled autologous responder T cells in ratios 1:0.5, 1:1 and 1:2 for patient 1 and in a ratio of 1:2 for patients 2 and 3. Anti-CD3/anti-CD28 beads (Life Technologies) were used as stimulus. CD4$^+$ cells were analyzed using FACSAria II flow cytometer (BD Biosciences). The suppression percentage was calculated with the following formula: 100- [(% proliferation in presence of T_{reg}/ % proliferation in absence of T_{reg})x100].[18]

Evaluation of T and NK cell responses is described in detail elsewhere.[17,19] For the assessment of T cell activation and degranulation, fresh mononuclear cells (MNCs) were stimulated for 6 h with anti-CD3, anti-CD28 and anti-CD49d (BD Biosciences). For NK cell degranulation, cytokine and cytotoxicity assays, fresh MNCs or FACS-sorted CD3$^-$CD16/56$^+$ NK cells were stimulated with K562 target cells for 6 h. The cells were analyzed using 4- or 6-color flow cytometry panel with mAbs against the antigens CD45, CD3, CD4, CD8, CD16, CD56, CD45, CD45RA, TCRγ, CCR7, IFN-γ and TNF. Additionally, standard 4 h chromium 51 (^{51}Cr)-release assays were performed according to established protocols for clinical samples using magnetic bead–separated CD3$^+$CD8$^+$ T cell or CD3$^-$CD56$^+$ NK cell subsets.[19,20]

Cytokine production

Whole blood was diluted 1:5 with Rosewell Park Memorial Institute medium (RPMI) into 96-well plates and activated by single stimulation or co-stimulations as indicated with IL-12 (20 ng/ml; R&D Systems; Abingdon), Phytohemagglutinin (PHA; 10 µg/ml; Sigma-Aldrich), LPS (1 µg/ml) List Biochemicals, IFN-y (2x10exp IU/ml, Immukin, Boehringer Ingelheim), IL-18 (20 ng/ml; R&D Systems; Abingdon), BCG (SSI; 3.4x10exp4/well), PMA (10ng/ml, Sigma), Ionomycin (1µg/ml; Sigma). Supernatants were taken at 24h. Cytokines were measured using standard ELISA according to the manufacturer's recommendations (IFN-y, Pelikine, Sanquin, NL), or multiplexed particle based flow cytometry (TNFa, IL-12, IL-10, IL-6, IL-17; R+D Systems Fluorokinemap) on a Luminex analyser (Bio-Plex, Bio-rad, UK)

For evaluation of IFN-γ signaling in monocytes, PBMNCs were plated in flat-bottomed 96-well plates (Costar Corning #3596) at $0.5x10^6$ cells / well and stimulated with IFN-γ (0.01 ng/ml – 150 ng/ml; Immunotools) for 60 min. PBMNCs were thereafter fixed, permeabilised, and stained with FITC- anti-CD14 (11-0149) and PE-anti-pSTAT1 (12-9008) antibodies according to manufacturer's protocol (eBioScience). STAT1 phosphorylation was determined in $CD14^+$ monocytes using flow cytometry. To assess TLR-signaling in monocytes, PBMNCs were stimulated with 100 ng/ml of LPS (Sigma Aldrich) or left unstimulated for 60 min. L-selectin shedding was determined from $CD14^+$ monocytes by flow cytometry with antibodies againstanti PE-anti-CD62L (12-9008) and FITC-anti-CD14 (11-0149). Flow cytometry was performed with Accuri cytometer and manufacturer's software (Becton Dickinson).

Anti-cytokine serology was performed by multiplexed particle-based flow cytometry as previously described.[21] Serum IgG antibodies to the following cytokines were investigated: IFN-γ, TNF, IL-12, IL-23, IFN-α, IFN-ω, IL-6, IL17A, IL17F, IL-22 and GM-CSF.

Immunohistochemical staining of phospho-STAT3 and cleaved caspase-3

Immunohistochemisty (IHC) of bone marrow (BM) biopsy paraffin sections was performed according to standard techniques using pSTAT3[Y705] mAb (9145S, Cell Signaling Technology) 1:100 and cleaved caspase-3 mAB (Cell Signaling Technology) 1:300. BM biopsy slides from 3 healthy individuals were used as controls.

Results

Gain-of function *STAT3* mutations are associated with multisystemic autoimmunity and mycobacterial disease

Patients 1 and 2 were recently shown to carry heterozygous, activating mutations in *STAT3*.[14] The mutations (p.K658N at chr17:40474427 C>G and p.K392R at chr17:40481630 T>C) localized to the *STAT3* Src-like homolog 2 (SH2) and DNA binding domains (Figure 2A-B). Exome sequencing was used to identify a novel *de novo* missense *STAT3* mutation at position chr17:40481624 A>G resulting in methionine-to-threonine substitution at position 394 (M394T) in the *STAT3* DNA binding domain in patient 3. To compare the functional effect of these mutations, we transiently transfected HEK293 cell line stably expressing luciferase under a STAT3-specific site-promoter with constructs encoding WT or mutated *STAT3*. For K392R and M394T mutations, we observed *STAT3* transcriptional activation under basal conditions suggesting that these mutants are constitutively active (Figure 2C). In case of K658N mutant there was no transcriptional activity under basal conditions, but the mutant showed higher *STAT3* transcriptional activation to low IL-6 concentrations than WT *STAT3*, the effect saturating in higher concentrations (Figure 2D).

Effects of *STAT3* mutations on STAT3 phosphorylation status

The phosphorylation of tyrosine residue 705 (pY705) of STAT3 is essential for the dimerization and activation of WT STAT3.[22] To evaluate whether the observed STAT3 hyperactivity was dependent on increased STAT3 phosphorylation, we used parallel-derived whole cell lysates of the transiently transfected HEK293 cells to determine the level of pSTAT3^{Y705} protein by western blotting both at baseline and after IL-6 stimulation. Expression of mutant pSTAT3^{Y705} was similar to WT (Figure 2E). Additionally, we assessed the expression of pSTAT3^{Y705} from fresh whole blood samples by FACS-based phosphoflow method (Figure 2F). The proportion of pSTAT3^{Y705}-positive lymphocytes ranged between upper normal to slightly increased in K392R and K658N mutated patients.

Additionally, bone marrow biopsies from patients 1 (K658N) and 2 (K392R) were stained for pSTAT3^{Y705} IHC. In both cases we observed increased number of pSTAT3^{Y705}-positive cells (Figure 3A-C). Morphologically the pSTAT3^{Y705}-positive BM-infiltrating cells were classified as LGLs. The number of pSTAT3^{Y705}-positive lymphocytes was higher in the patient 2 carrying the

K392R mutation, which could be related to the recently made T-LGL leukemia diagnosis (Figure 3A-B).

STAT3 hyperactivity is associated with peripheral eosinopenia, hypogammaglobulinemia and deficiency of T$_{reg}$, NK and dendritic cells

The effects of the *STAT3* mutations K392R, K658N and M394T on the properties, phenotype, and functionality of hematopoietic cells were analyzed in detail using IHC and flow cytometry (Table 2, Figure 1C). In the myeloid lineage of patients 1 (K658N) and 2 (K392R), we observed marked peripheral eosinopenia with modest BM eosinophilia, suggesting an eosinophil mobilization defect. The BM biopsies from both patients were stained with cleaved caspase-3 antibody to detect increased eosinophil apoptosis, but the results were comparable to healthy controls (data not shown). We also noted plasmacytoid dendritic cell (DC) deficiency in all patients. The other cells of the myeloid lineage showed normal maturation in the BM and normal peripheral blood counts.

The results of the lymphoid lineage analysis are presented in Table 2. The patients had normal overall CD3$^+$CD4$^+$ and CD3$^+$CD8$^+$ T cell and CD19$^+$ B cell counts but low relative CD3$^-$CD16$^+$CD56$^+$ NK cell counts. In the more detailed analyses of cytotoxic lymphocyte subsets, the frequencies of early differentiated CD56^{bright} and late differentiated CD57$^+$ NK cells were normal. The patients' NK cells expressed normal levels of cytotoxic granule constituents perforin, granzyme A, and granzyme B (data not shown). Moreover, NK cell and cytotoxic CD3$^+$CD8$^+$CD57$^+$ T cell degranulation and target cell killing were also within normal range, as was IFN-γ and TNF production in response to engagement of ITAM-coupled activating receptors (data not shown). NK cell killing of K562 target cells was also assessed and found to be within normal range (data not shown).

Over time, all patients developed unspecific hypogammaglobulinemia or antibody deficiency (Table 2). In B cell subset analyses, the relative numbers of activated CD19$^+$CD38^{low}CD21^{low} B cells and CD19$^+$CD21$^+$ mature B cells were increased. Additionally, a rise in marginal zone-like CD19$^+$CD27$^+$IgD$^+$IgM$^+$ B cells with a corresponding decrease in CD19$^+$CD27$^+$IgD$^-$IgM$^-$ switched memory B cells was observed. The patients were screened for autoantibodies against endocrine and exocrine organs as well as intracellular proteins (for a detailed account see Supplementary table S2). Patient 1 had positive anti-thyroid peroxidase (TPO) antibodies without clinical thyroid disease. Patient 2 had high titer diabetes autoantibodies. All other autoantibody titers were negative.

In the T cell compartment, we noticed a deficiency of $CD4^+CD25^+FOXP3^+$ T_{regs} in the IPEX-like patients 1 and 2 (Table 2). Also, the suppressive capacity of T_{reg} cells was reduced (Supplementary Figure 2). In patient 3, T_{reg} cell counts and suppressive capacity were comparable to the controls. Surprisingly, the proportions of IL-17 producing $CD4^+CD69^+$ Th17 cells were also decreased in all patients. To confirm the finding, the production of IL-17 upon PHA-stimulation was assessed by multiplexed particle based flow cytometry in patient 3. This showed minimal response (Supplementary Figure 5).

Intact cytokine production in M394T-mutated patient with mycobacterial disease

Patient 3 with the *STAT3* M394T mutation developed disseminated mycobacterial disease in late adolescence. Since Mendelian susceptibility to mycobacterial disease generally involves defects in IL-12/IFN-γ feedback loop,[23] the pathway was extensively tested but found normal. IFN-γ-receptor–STAT1 signaling was intact, since STAT1 phosphorylation and upregulation of HLA-DR expression followed normal dose-response curves after *in vitro* stimulation with IFN-γ (data not shown). There was normal LPS-induced shedding of L-selectin (CD62L) suggesting normal TLR signaling (data not shown).

Release of IL-12, TNF and IFN-γ was normal after stimulation of PBMNC with T-cell specific antigens. Notably, upon stimulation of PBMNC with IL-12 plus LPS or IL-18, IFN-γ production was very low (Supplementary figure 5). These results suggested a defect in NK cell-mediated release of IFN-γ. However, flow cytometric assessment of intracellular IFN-γ production revealed normal production of IFN-γ on a per cell basis (data not shown). Therefore, the reduced release of IFN-γ likely reflected the overall low frequency of NK cells among PBMNC rather than a defect in NK cell function *per se*. The patient was also tested negative for autoantibodies against various cytokines including IFN-γ, TNF, IL-12, IL-23, IFN-α, IFN-ω, IL-6, IL17A, IL17F, IL-22 and GM-CSF (data not shown).

K392R-mutated patient developed T cell LGL leukemia

Patient 2 with the STAT3 K392R mutation developed aberrant LGL proliferation, which was associated with megaloblastic anemia. In the detailed T cell subset analysis, the phenotype of the abnormal cells was $CD3^+TCR-γδ^+$, and they accounted for 57% of all $CD3^+$ T cells (Figure 3D-F). However, the $CD3^+TCR-γδ^+$ population was not homogenous: 45 % of the cells were $CD8^+$

12

whereas the rest had TCR-$\gamma\delta^+$CD4$^-$CD8$^-$ immunophenotype (Figure 3D-F). The clonality of the LGL proliferation was confirmed by the positive result of a routine clinical TCR-$\gamma\delta$ receptor PCR analysis. Since the LGL proliferation mainly consisted of CD4$^-$CD8$^-$ cells, we reviewed the patients' earlier CD4$^-$CD8$^-$ counts. All patients' proportions of CD3$^+$CD4$^-$CD8$^-$ T cells were above median (Table 2), but only in the K392R-mutated patient they were predominantly $\gamma\delta$ T cells.

No cytogenetic alterations were found in the LGL-subset in routine clinical investigations. To elucidate potential oncogenic single nucleotide variants (SNVs) driving the LGL expansion, the CD3$^+$TCR $\gamma\delta$ cells were exome sequenced in parallel with the germline DNA extracted from saliva sample. Four novel somatic mutations were called in the following genes*: LY9, RB1CC1, FOXP4* and *ICOSLG* (Table 3). The variant allele frequency varied between 10-17%, suggesting that the mutations were located in a subpopulation of TCR-$\gamma\delta^+$ cells. No loss of heterozygosity for the germline *STAT3* K392R mutation was observed, and no genomic rearrangements were detected.

Discussion

In this study, we identified activating germline *STAT3* mutations K658N,[14] K392R[14] and M394T in three patients with autoimmunity, hypogammaglobulinemia, lymphoproliferation and mycobacterial disease. Autoimmunity and hypogammaglobulinemia were seen in all cases, and the displayed autoimmune phenomena are distinctly rare in children (desquamative interstitial pneumonitis, posterior uveitis). Lymphoproliferation (lymphadenopathy, splenomegaly or pediatric T-LGL leukemia) was present in two cases. One patient developed disseminated mycobacterial disease in late adolescence. The patients presented with somewhat high proportions of $CD3^+CD4^-CD8^-$ T cells with decreased counts of dendritic, T_{reg}, Th17 and NK cells as well as deficiency of switched memory B cells.

Heterozygous loss-of-function *STAT3* mutations have been associated with autosomal dominant HIES, which is characterized by high serum IgE, eosinophilia, eczema and immunodeficiency.[5,6] Our first patient developed eczema that differed from the typical hyper-IgE eczema clinically and histopathologically (data not shown). All patients were susceptible to respiratory infections, partly due to their hypogammaglobulinemia. No other features of HIES were noted. The mutations in HIES localize to the DNA-binding and SH2 domains of STAT3, whereas the observed activating *STAT3* mutations scatter throughout the protein.[5,6,14] Mutations in the DNA binding domain caused constitutive activation of STAT3, whereas the K658N mutation in the dimerization domain only conferred hypersensitivity to interleukins. The difference in action however does not correlate with the phenotype. It is possible that under physiologic conditions, hypersensitivity to low levels of interleukins is sufficient for persistent activation of STAT3 signaling.

Autoimmunity is commonly seen in patients with germline *STAT* mutations, sometimes with concomitant T_{reg} deficiency.[2,3] (For comparison between IPEX-like syndromes caused by *STAT1*, *STAT3*, and *STAT5B* mutations see supplementary table S5). STAT3 promotes the activation and expansion of autoimmunity-associated Th17 cells, whereas STAT5 drives the immunosuppressive T_{reg} fate. STAT3 and STAT5b bind to multiple sites of the IL-17 locus, with STAT3 binding promoting IL-17 transcription, and STAT5b binding conversely repressing IL-17 transcription.[24,25] Th17 deficiency is seen in loss-of-function *STAT3* mutations and HIES.[26,27] Curiously, our patients with activating *STAT3* mutations presented also with a reduced number of Th17 cells and decreased IL-17 production.

A notable feature of the STAT3 hyperactivity patients was lymphoproliferation, which has not been described in other IPEX-like syndromes.[3] The somewhat elevated CD4$^-$CD8$^-$ T cell counts observed in our patients may suggest a defect in the lymphocyte apoptosis.[28] Notably, patient 2 (K392R) developed T-LGL leukemia at age 14. LGL leukemia is mainly diagnosed in the elderly and is often accompanied by autoimmune processes such as rheumatoid arthritis and autoimmune cytopenias. Somatic *STAT3* gain-of-function mutations have been identified in 40-70% of T cell LGL leukemia cases.[11-13] The occurrence of pediatric LGL leukemia in patient 1 and the presence of LGL-like cells in the bone marrow of patient 2 suggest *STAT3* is to be a central oncogene in LGL leukemia pathogenesis.

Patient 3 (M394T) presented only mild autoimmunity but developed disseminated mycobacterial disease in late adolescence. In contrast to most known mycobacterial susceptibility syndromes,[23] IL-12-IFN-γ signaling was not impaired. Dendritic cell deficiencies cause mycobacterial disease,[29] and the observed lack of plasmacytoid dendritic cells may partly explain her condition. Why our IPEX-like patients have not developed mycobacterial infections is unknown. Since dendritic cell deficiency -associated mycobacterial disease is often late-onset, their young age might provide an explanation.

In conclusion, activating germline *STAT3* mutations lead to broad range of immune disturbances including multi-organ autoimmunity, lymphoproliferation, hypogammaglobulinemia, and delayed -onset mycobacterial disease. Emerging STAT3 inhibitors, some of which are in clinical trials, may benefit such patients. Our results provide insights into the role of STAT3 in the pathogenesis of autoimmune diseases and highlight the oncogenic nature of STAT3 in LGL leukemia development.

Acknowledgements

Author contributions

E.H. designed the study, coordinated the project, analyzed the data and wrote the paper. M.K. and H.L.M.R. contributed to writing of the paper and performed laboratory analysis. S.M., M.S., J.S. and J.K. designed and supervised the study, reviewed the data and contributed to writing of the paper. Y.T.B., S.C., V.G., P.K., S.S., H.K., A.A., R.D. and A.H. designed and performed laboratory analysis. S.E., L.T. and R.K. designed and performed bioinformatics analysis. M-L.K-L. and P.E.K. reviewed the immunopathology. T.H-K., T.O., M.S., K.P., R.U-S., L.K. and K.H. provided clinical care for the patients. All authors read and approved the final manuscript.

Disclosure of Conflicts of Interest

K.P. has received research funding and honoraria from Novartis and Bristol-Myers Squibb. S.M. has received honoraria from Novartis and Bristol-Myers Squibb. M.S. has received honoraria from Octapharma and Sanquin.

References

1.   Bennett CL, Christie J, Ramsdell F, et al. The immune dysregulation, polyendocrinopathy, enteropathy, X-linked syndrome (IPEX) is caused by mutations of FOXP3. *Nat Genet*. 2001;27(1):20-21.

2.   Uzel G, Sampaio EP, Lawrence MG, et al. Dominant gain-of-function STAT1 mutations in FOXP3 wild-type immune dysregulation-polyendocrinopathy-enteropathy-X-linked-like syndrome. *J Allergy Clin Immunol*. 2013;131(6):1611-1623.

3.   Verbsky JW, Chatila TA. Immune dysregulation, polyendocrinopathy, enteropathy, X-linked (IPEX) and IPEX-related disorders: an evolving web of heritable autoimmune diseases. *Curr Opin Pediatr*. 2013;25(6):708-714.

4.   Lohr NJ, Molleston JP, Strauss KA, et al. Human ITCH E3 ubiquitin ligase deficiency causes syndromic multisystem autoimmune disease. *Am J Hum Genet*. 2010;86(3):447-453.

5.   Holland SM, DeLeo FR, Elloumi HZ, et al. STAT3 mutations in the hyper-IgE syndrome. *N Engl J Med*. 2007;357(16):1608-1619.

6.   Minegishi Y, Saito M, Tsuchiya S, et al. Dominant-negative mutations in the DNA-binding domain of STAT3 cause hyper-IgE syndrome. *Nature*. 2007;448(7157):1058-1062.

7.   Dupuis S, Jouanguy E, Al-Hajjar S, et al. Impaired response to interferon-alpha/beta and lethal viral disease in human STAT1 deficiency. *Nat Genet*. 2003;33(3):388-391.

8.   Liu L, Okada S, Kong XF, et al. Gain-of-function human STAT1 mutations impair IL-17 immunity and underlie chronic mucocutaneous candidiasis. *J Exp Med*. 2011;208(8):1635-1648.

9.   Knosp CA, Johnston JA. Regulation of CD4+ T-cell polarization by suppressor of cytokine signalling proteins. *Immunology*. 2012;135(2):101-111.

10.   O'Shea JJ, Plenge R. JAK and STAT signaling molecules in immunoregulation and immune-mediated disease. *Immunity*. 2012;36(4):542-550.

11.   Jerez A, Clemente MJ, Makishima H, et al. STAT3 mutations unify the pathogenesis of chronic lymphoproliferative disorders of NK cells and T-cell large granular lymphocyte leukemia. *Blood*. 2012;120(15):3048-3057.

12.   Koskela HL, Eldfors S, Ellonen P, et al. Somatic STAT3 mutations in large granular lymphocytic leukemia. *N Engl J Med*. 2012;366(20):1905-1913.

13.   Fasan A, Kern W, Grossmann V, Haferlach C, Haferlach T, Schnittger S. STAT3 mutations are highly specific for large granular lymphocytic leukemia. *Leukemia*. 2013;27(7):1598-1600.

14.   Flanagan SE, Haapaniemi E, Russell MA, et al. Activating germline mutations in STAT3 cause early-onset multi-organ autoimmune disease. *Nat Genet*. 2014;46(8):812-814.

15.   Otonkoski T, Roivainen M, Vaarala O, et al. Neonatal Type I diabetes associated with maternal echovirus 6 infection: a case report. *Diabetologia*. 2000;43(10):1235-1238.

16.   Sulonen AM, Ellonen P, Almusa H, et al. Comparison of solution-based exome capture methods for next generation sequencing. *Genome Biol*. 2011;12(9):R94.

17.   Ilander M, Kreutzman A, Rohon P, et al. Enlarged Memory T-Cell Pool and Enhanced Th1-Type Responses in Chronic Myeloid Leukemia Patients Who Have Successfully Discontinued IFN-alpha Monotherapy. *PLoS One*. 2014;9(1):e87794.

18.   Ruitenberg JJ, Boyce C, Hingorani R, Putnam A, Ghanekar SA. Rapid assessment of in vitro expanded human regulatory T cell function. *J Immunol Methods*. 2011;372(1-2):95-106.

19.   Chiang SC, Theorell J, Entesarian M, et al. Comparison of primary human cytotoxic T-cell and natural killer cell responses reveal similar molecular requirements for lytic granule exocytosis but differences in cytokine production. *Blood*. 2013;121(8):1345-1356.

20.   Schneider EM, Lorenz I, Muller-Rosenberger M, Steinbach G, Kron M, Janka-Schaub GE. Hemophagocytic lymphohistiocytosis is associated with deficiencies of cellular cytolysis but normal expression of transcripts relevant to killer-cell-induced apoptosis. *Blood*. 2002;100(8):2891-2898.

21.   Puel A, Doffinger R, Natividad A, et al. Autoantibodies against IL-17A, IL-17F, and IL-22

in patients with chronic mucocutaneous candidiasis and autoimmune polyendocrine syndrome type I. *J Exp Med*. 2010;207(2):291-297.

22.   Bromberg JF, Wrzeszczynska MH, Devgan G, et al. Stat3 as an oncogene. *Cell*. 1999;98(3):295-303.

23.   Cottle LE. Mendelian susceptibility to mycobacterial disease. *Clin Genet*. 2011;79(1):17-22.

24.   Yang XO, Panopoulos AD, Nurieva R, et al. STAT3 regulates cytokine-mediated generation of inflammatory helper T cells. *J Biol Chem*. 2007;282(13):9358-9363.

25.   Yang XP, Ghoreschi K, Steward-Tharp SM, et al. Opposing regulation of the locus encoding IL-17 through direct, reciprocal actions of STAT3 and STAT5. *Nat Immunol*. 2011;12(3):247-254.

26.   Minegishi Y, Saito M, Nagasawa M, et al. Molecular explanation for the contradiction between systemic Th17 defect and localized bacterial infection in hyper-IgE syndrome. *J Exp Med*. 2009;206(6):1291-1301.

27.   de Beaucoudrey L, Puel A, Filipe-Santos O, et al. Mutations in STAT3 and IL12RB1 impair the development of human IL-17-producing T cells. *J Exp Med*. 2008;205(7):1543-1550.

28.   Magerus-Chatinet A, Stolzenberg MC, Loffredo MS, et al. FAS-L, IL-10, and double-negative CD4- CD8- TCR alpha/beta+ T cells are reliable markers of autoimmune lymphoproliferative syndrome (ALPS) associated with FAS loss of function. *Blood*. 2009;113(13):3027-3030.

29.   Collin M, Bigley V, Haniffa M, Hambleton S. Human dendritic cell deficiency: the missing ID? *Nat Rev Immunol*. 2011;11(9):575-583.

Tables

Table 1. Clinical manifestations of STAT3 gain-of-function patients.

	PATIENT 1	PATIENT 2	PATIENT 3
STAT3 mutation	K658N	K392R	M394T
Sex	Female	Female	Female
Age (years)	17	15	22
Birthweight (SD)	0	-5	0
Growth (SD), puberty	-4 Delayed puberty	-7 Delayed puberty	0 Normal puberty
Infection susceptibility	Upper respiratory tract infections Severe dental caries Severe varicella	Lower respiratory tract infections Severe dental caries	Non-tuberculous mycobacteria Lower respiratory tract infections
Endocrine	Subclinical hypotyreosis with TPO positivity	Neonatal diabetes with positive IAA/GADA/ICA autoantibodies	-
Gastrointestinal	Autoimmune enteropathy	Coeliac disease Rudimentary pancreas	Lymphocytic colitis
Skin	Generalized, livedo-like exfoliating dermatitis	-	Mild atopic-like eczema
Pulmonary	Cryptogenic organising pneumonia, asthma-like symptoms, bronchiectasis	Desquamative interstitial pneumonitis	Non-tuberculous mycobacteria
Hematology	Lymphadenopathy consisting of polyclonal CD4$^+$ cells hepatosplenomegaly Bone marrow eosinophilia Autoimmune hemolytic anemia	T-cell LGL leukemia Bone marrow eosinophilia Autoimmune hemolytic anemia	Immune thrombocytopenia
Autoinflammation	Sterile pleuritis or serositis with high fever and elevated inflammatory markers	-	-
Other	Sicca syndrome and bilateral	Severe allergy	-

19

	posterior uveitis with cystic macular edema		

Abbreviations: SD, Standard Deviation; IAA, Insulin autoantibodies; GADA, Glutamic acid decarboxylase autoantibodies; ICA, Islet cell autoantibodies

Table 2. Immunologic features of patients with STAT3 gain-of-function mutations.

		Normal range / Healthy control median value	Patient 1 (K658N)	Patient 2 (K392R)	Patient 3 (M394T)
Leukocytes		*3400-8200*	*7100*	*6900 (7500)**	*5900*
	Lymphocytes	1000-4500	1700	4278 (1270)*	820 ↓
	Monocytes	200-800	600	690 (370)*	570
	Neutrophils	1500-7500	4800	1750 (5830)*	4130
	Basophils	0-100	0	182 (0)*	80
	Eosinophils	100-400	0 ↓	10 (0)*↓	280
	platelets	150000-360000	267000	290000 (266000)*	271000
	NK-cells (CD3$^-$CD16$^+$/56$^+$)	90-600 (12%)	12 (0.7%) ↓	128 (3%) (38, 0.5%)* ↓	40-90(4-13%) ↓
	NK cell function and maturation		normal	normal	normal
Dendritic cells					
Plasmacytoid	lin$^-$HLA-DR$^+$CD123$^+$CD11c$^-$	*0.1-0.3%*	0.06 % ↓	<0.01% ↓	0.01% ↓
Monocytoid	lin$^-$HLA-DR$^+$CD123$^-$CD11c$^+$	*0.1-0.3%*	0.2 %	<0.01% ↓	0.73% ↑
CD3$^+$ T cells		*700-2100 (71%)*	*1462 (86%)*	*3507 (82%) (1092, 86%)**	*474 (74%)*
	TCRαβ$^+$	94%	94%	45% ↓ (93%)*	97%
	TCRγδ$^+$	6%	6%	55% ↑ (7%)*	3%
	CD57$^+$	21%	8.4%	65% ↑	65% ↑
	CD4$^-$CD8$^-$	4.2%	3.4%	30% (2.3%)* ↑	6 %
	CD4$^-$CD8$^-$ TCRαβ$^+$	<3.4%	1.6 %	1 %	5%↑
	CD4-CD8- TCRγδ +	NA	1.8 %	29 %↑	1%
CD3$^+$CD4$^+$ T cells		*458-1406 (60%)*	*789 (54%)*	*666 (19%)↓ (380, 34.8%)**	*307 (48%) ↓*
	CD45RO$^+$	51 %	46 %	70% ↑	NA
	CD45RA$^+$	47 %	51 %	26% ↓	18% ↓
	Ki-67$^+$	2 %	2,50 %	1.80 %	NA
	HLA-DR$^+$	3 %	29 %	1.90 %	NA
TCM	CCR7$^+$CD45RA$^-$	38 %	44 %	54% ↑	56% ↑
Naive	CCR7$^+$CD45RA$^+$	45 %	50 %	24% ↓	20% ↓
TEM	CCR7$^-$CD45RA$^-$	11 %	5 %	22% ↑	23% ↑
Temra	CCR7$^-$CD45RA$^+$	4 %	1 %	1 %	2%
	Granzyme B$^+$	1 %	0.2 %	1.9 %	NA
unstimulated	IFNγ/TNFα secretion	0 %	0.2 %	0.1 %	normal§
stimulated	IFNγ/TNFα secretion	5 %	7.3 %	21.5% ↑	normal§
T$_{reg}$	FOXP3$^+$CD25$^+$	2.3-7.8%	1.45% ↓	(0.67%)* ↓	4.9%
T$_{reg}$ suppressive capacity			low	low	normal
Th17 †	CD69$^+$IL17$^+$	0.47-1.59%	0.13% ↓	(0.35%)* ↓	0.22 ↓
CD3+CD8+ T-cells		*200-1200 (51%)*	*570 (39%)*	*1790 (51%) (339, 31%)**	*134 (21%)*
	CD45RO$^+$	41 %	20 %	5% ↓	NA
	CD45RA$^+$	72 %	76 %	93% ↑	68%
	Ki-67$^+$	1 %	2,70 %	16% ↑	NA
	HLA-DR$^+$	3 %	29 %	56% ↑	NA
TCM	CCR7$^+$CD45RA$^-$	8 %	11 %	3 %	13%
Naive	CCR7$^+$CD45RA$^+$	35 %	62% ↑	8% ↓	45% ↑
TEM	CCR7$^-$CD45RA$^-$	27 %	8% ↓	4% ↓	22%
Temra	CCR7$^-$CD45RA$^+$	33 %	19 %	86% ↑	21%

21

	Granzyme B$^+$	11 %	14,9 %	0.2 %	NA
unstimulated	IFNγ/TNFα secretion	0 %	0,1 %	0.1 %	normal§
stimulated	IFNγ/TNFα secretion	7.20 %	4.50 %	4.30 %	normal§
CD19+ B-cells		*70-230 (12%)*	*660 (9.3%)*	*174 (14%)**	*80 (11%)*
Transitional	CD38^{hi}IgM^{hi}	0.6-3.5%	3.4%	(0%)* ↓	0.4% ↓
Naive	CD27$^-$IgD$^+$	NA	70% ↑	(68%)*↑	94% ↑
Mature B-cells	CD21$^+$	11-45%	84 % ↑	(70%)* ↑	88 ↑
Memory	CD27$^+$	15-45%	23 %	(26 %)*	4% ↓
Marginal zone-like	CD27$^+$IgD$^+$IgM$^+$	7.2-30.8%	19.5% ↑	(24.9%)* ↑	2.9%
Switched memory	CD27$^+$IgD$^-$IgM$^-$	6.5-29.2%	0.5% ↓	(0.5%)* ↓	<0.1 ↓
Plasmablasts	CD38^{++}IgM$^-$	-	0.0%	(0.37%)*	0.5
Activated	CD38^{low}CD21^{low}	0.6-3.5%	12.1% ↑	(22.5%)* ↑	11.7↑
Immunoglobulins (prior IVIG)					
	IgG	6.8-15.0 g/L	5.8↓	2.8↓	0.16↓
	IgA	0.52-4.02 g/L	1.67	0.21	1.7
	IgM	0.47-2.84 g/L	3.38	1.44	0.6
	IgE	0-110 IU/L	0.7	0.5	<2
Complement	Classical., alternative and mannan-binding lectin pathway hemolytic activities	normal	normal	normal	
Lymphocyte proliferative responses to mitogens	Phytohemagglutinin, concanavalin A, pokeweed mitogen	normal	normal	normal	
Lymphocyte chemotaxis		NA	NA	normal	
Specific antibodies against vaccine antigens	Tetanus, diphtheria, pneumococcal polysaccharide	protective	protective	tetanus unprotective, others NA	
Autoantibodies ‡		TPO +	negative	negative	

CD3$^+$ T-cell, CD4$^+$ cell, CD8$^+$ cell and CD19$^+$ cell numbers are indicated as absolute counts and relative percentages of all lymphocytes (%). Healthy control values are indicated either as absolute count ranges or medians (%). Abbreviations: TCM, Central memory T-cell; TEM, Effector memory T-cell; Temra, Effector memory RA T-cell; Treg, Regulatory T-cell; IVIG, intravenous immunoglobulin therapy; TPO, Anti-thyroid peroxidase antibody; NA, Not applicable,
↑ High value, ↓ low value, ()* tested before onset of lymphoproliferation at 12 years of age, † of all activated CD3$^+$CD4$^+$ cells, ‡ for detailed specification see supplementary data, § test method differs from other patients

Table 3. Somatic mutations in the LGL clone of patient 2.

Gene	Chromosome	Position	Ref.base	Var.base	Amino acid change	Allele frequency (%)	Sift/Poly-Phen prediction	Somatic P-value[1]
LY9	1	160788035	T	C	I457T	17.27	Tolerated/benign	8.97×10^{-6}
RB1CC1	8	53570332	G	C	P686R	10.29	Tolerated/benign	0.00097
FOXP4	6	41533673	G	A	A59T	14.04	Tolerated/benign	0.003229
ICOSLG	21	45649510	A	G	L442P	14.04	Tolerated/benign	0.005479

Abbreviations: Ref, reference; Var, variant.

[1]Somatic p value for somatic/loss of heterozygosity events.

Figure legends

Figure 1. Clinical characteristics of patients. A. Livedo-like generalized exfoliating dermatitis in patient 1. The rash culminates in limb extensor areas. B. High-resolution computerized tomography of patient 2 showing ground-glass opacity, bronchoalveolar thickening and increased nodularity. C. Bone marrow biopsy from patient 1 showing modest bone marrow eosinophilia despite observed peripheral eosinopenia (yellow asterisks). HE stain, 40x magnification.

Figure 2. *STAT3* mutations K658N, K392R, and M394T in studied patients. A. Schematic representation of STAT3 protein domains with the observed mutations marked as black lines. Germ-line and somatic mutation hotspots for Hyper-IgE syndrome[5,6] and LGL leukemia[11-13] are indicated as green and blue bars above, respectively. B. Crystallographic structure of STAT3 dimer (the RCSB Protein Data Bank code 1BG1). K658N, K392R, and M394T mutations are indicated as red dots. C-D. HEK293 cells containing STAT3-responsive luciferase were transfected with empty, wild type and mutant STAT3 overexpression plasmids with or without IL-6 stimulation. The K392R and M394T significantly increased STAT3 transcriptional activity in basal and stimulated conditions. Error bars represent SEM (n=6, panel C). The K658N mutant showed hypersensitivity to IL-6 stimulation in low concentrations. Error bars represent SEM (n=3, panel D). 2 way ANOVA, * = $p<0.05$, ** = $p<0.01$ and *** = $P<0.001$. E. No significant increase in pSTAT3^{Y705} phosphorylation was observed when HEK293 cells were transfected with mutant STAT3 overexpression constructs. Equal amounts of parallel-derived whole cell lysates were loaded per condition. α-tubulin and STAT3 were used as loading and expression controls, respectively. + and – signs indicate presence and absence of IL-6 stimulation. F. In peripheral blood, no significant increase in STAT3 phosphorylation was noted in studied patients. Color change indicates relative pSTAT3^{Y705} expression. Forward panel: K392R, middle panel, K658N, back panel: healthy control (n=3, value range presented in brackets).

Figure 3. Abnormal lymphocyte populations detected in STAT3-mutated patients. Figures A-C: Bone marrow biopsy shows abnormally high number of phospho-STAT3 positive lymphocytes both in patient 2 (p.K392R) (A) but also, to a lesser extent, in patient 1 (p.K658N) (B). Patient 3 (M394T) was not available for study. In healthy bone marrow, no phospho-STAT3 cells are present (C). Figures 3D-F: Flow cytometry results from patient 2 (p. K392R). Majority of lymphocytes were CD3$^+$ (A) with 57% of the population expressing TCR-γδ (B). The TCR-γδ+ population consisted of CD4$^-$CD8$^-$ and CD4$^-$CD8$^+$ T-cells. The expression of TCR-γδ was considerably lower

in CD4⁻CD8⁻ cells than in CD4⁻CD8⁺ T-cells and therefore two populations are seen in the scatter plot. (C). In healthy individuals, TCR-γδ-expressing T-cells account less than 6% of all CD3+ T-cells and the TCR-γδ expression is normally uniform. 40x magnification, HE stain.
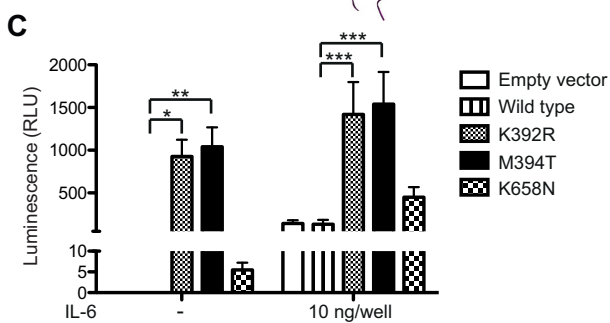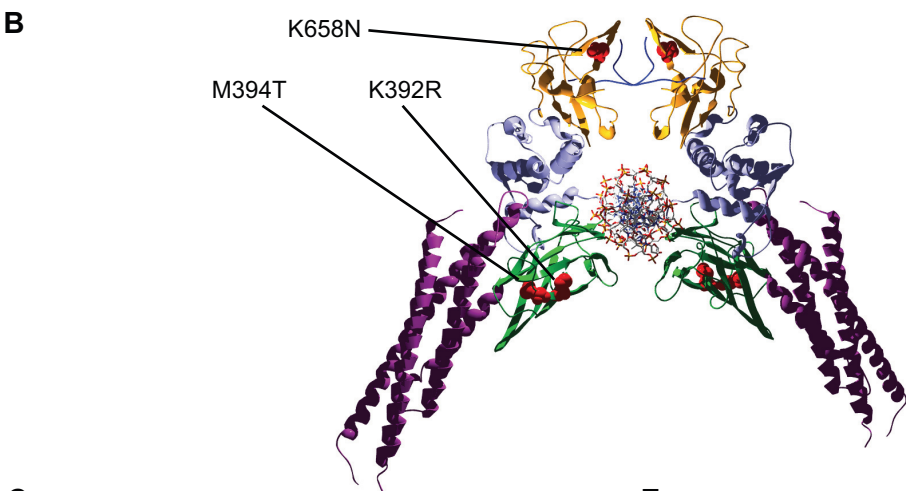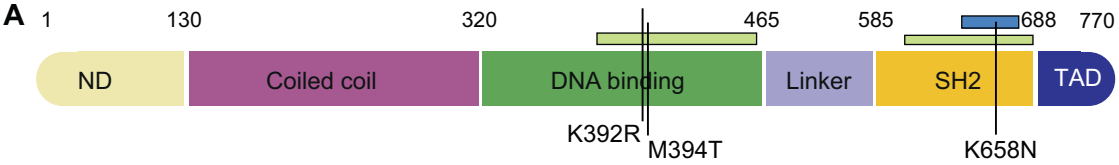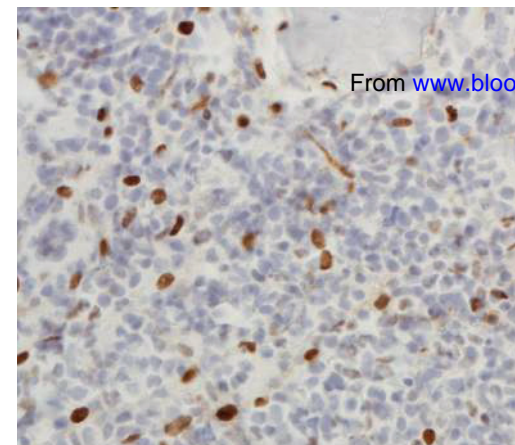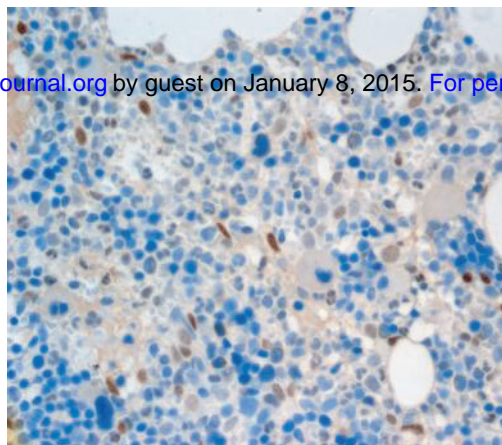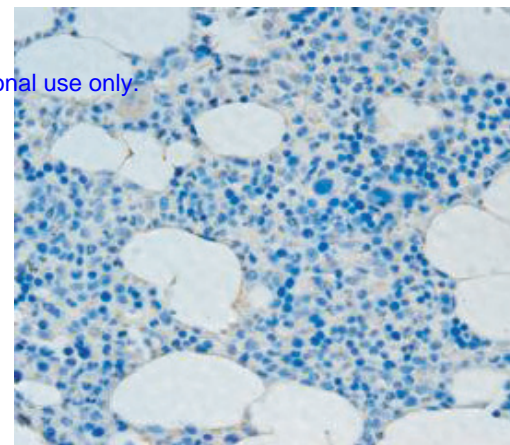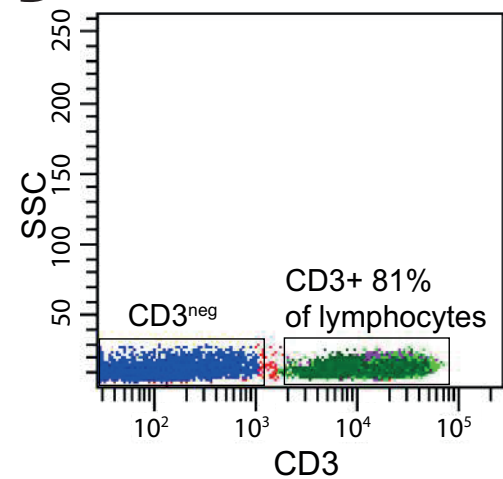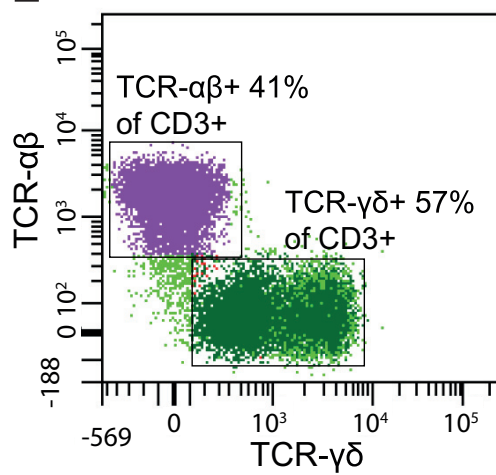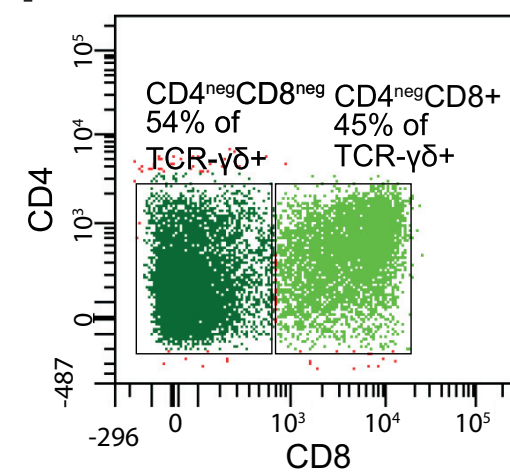
Figure 1

A
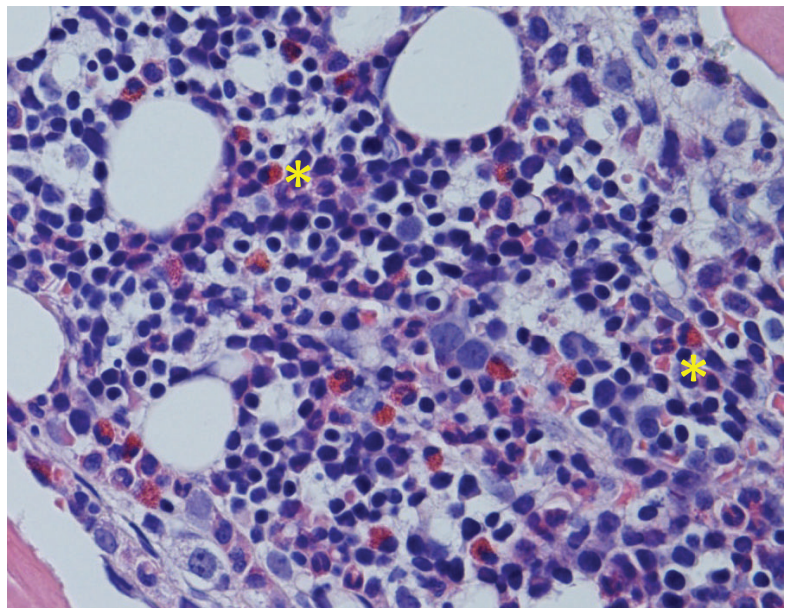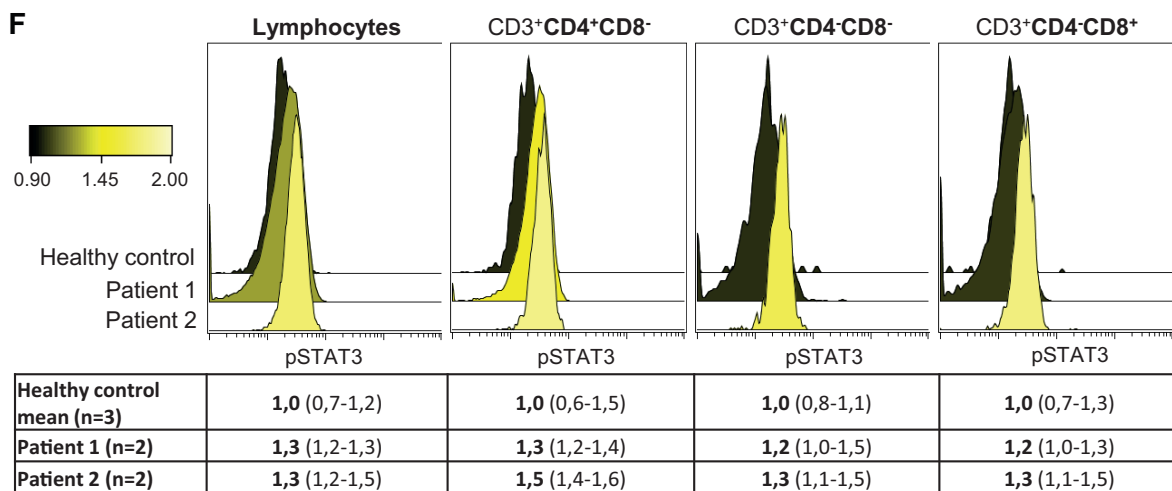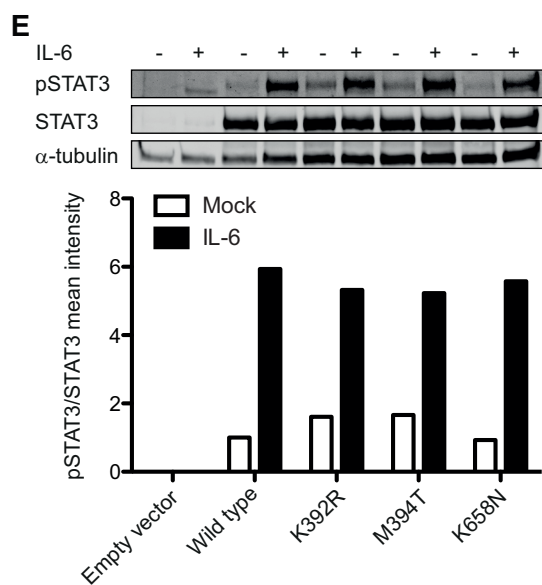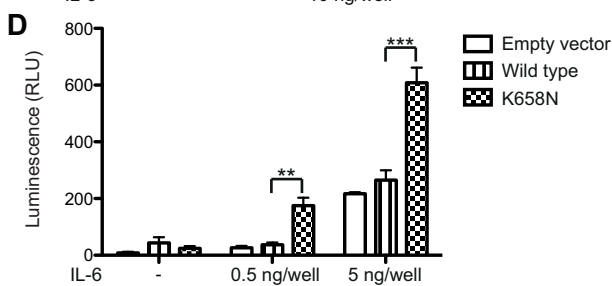
B

C

Figure 3

blood

Autoimmunity, hypogammaglobulinemia, lymphoproliferation and mycobacterial disease in patients with dominant activating mutations in *STAT3*

Emma M. Haapaniemi, Meri Kaustio, Hanna L.M. Rajala, Arjan J. van Adrichem, Leena Kainulainen, Virpi Glumoff, Rainer Doffinger, Heikki Kuusanmäki, Tarja Heiskanen-Kosma, Luca Trotta, Samuel Chiang, Petri Kulmala, Samuli Eldfors, Riku Katainen, Sanna Siitonen, Marja-Liisa Karjalainen-Lindsberg, Panu E. Kovanen, Timo Otonkoski, Kimmo Porkka, Kaarina Heiskanen, Arno Hänninen, Yenan T. Bryceson, Raija Uusitalo-Seppälä, Janna Saarela, Mikko Seppänen, Satu Mustjoki and Juha Kere

Information about reproducing this article in parts or in its entirety may be found online at:
http://www.bloodjournal.org/site/misc/rights.xhtml#repub_requests

Information about ordering reprints may be found online at:
http://www.bloodjournal.org/site/misc/rights.xhtml#reprints

Information about subscriptions and ASH membership may be found online at:
http://www.bloodjournal.org/site/subscriptions/index.xhtml